2556 *Organometallics* **2000,** *19,* 2556−2563

Unexpected P−Si or P−C Bond Cleavage in the Reaction of $Li_2[(C_5Me_4)SiMe_2PR]$ (R = Cyclohexyl, 2,4,6-$Me_3C_6H_2$) and $Li[(C_5H_4)CMe_2PHR]$ (R = Ph, ^tBu) with $ZrCl_4$ or $[TiCl_3(thf)_3]$: Formation and Molecular Structure of the *ansa*-Metallocenes $[\{(\eta\text{-}C_5Me_4)_2SiMe_2\}ZrCl_2]$ and $[\{(\eta\text{-}C_5H_4)_2CMe_2\}MCl_2]$ (M = Ti, Zr)[†]

Thomas Koch, Steffen Blaurock, Fernando B. Somoza, Jr., Andreas Voigt,
Reinhard Kirmse, and Evamarie Hey-Hawkins*

Institut für Anorganische Chemie der Universität, D-04103 Leipzig, Germany

Received September 28, 1999

The (phosphinosilyl)cyclopentadiene 1-$SiMe_2PHMes$-2,3,4,5-Me_4C_5H, prepared from 1-$SiMe_2Cl$-2,3,4,5-Me_4C_5H and LiPHMes (Mes = 2,4,6-$Me_3C_6H_2$), reacts with MeLi to yield $Li_2[(C_5Me_4)SiMe_2PMes]$ (**2**). The (phosphinomethyl)cyclopentadienide $Li[(C_5H_4)CMe_2PH^tBu]$ (**4**) is obtained by the reaction of $LiPH^tBu$ with 6,6-dimethylfulvene. $Li_2[(C_5Me_4)SiMe_2PR]$ (R = cyclohexyl (Cy; **1**), Mes (**2**)) reacts in situ with $ZrCl_4$ at −30 °C to give $[\{(\eta\text{-}C_5Me_4)_2SiMe_2\}ZrCl_2]$ (**5**). The formation of $(PCy)_4$ and $(PHMes)_2$, respectively, in these reactions was shown by ^{31}P NMR spectroscopy. In the reaction of $Li[(C_5H_4)CMe_2PHR]$ (R = Ph (**3**), ^tBu (**4**)) with $ZrCl_4$ or $[TiCl_3(thf)_3]$, $[\{(\eta\text{-}C_5H_4)CMe_2PHR\}_2ZrCl_2]$ (R = Ph (**6**), ^tBu (**7**)) and $[\{(\eta\text{-}C_5H_4)CMe_2PHR\}_2TiCl]$ (R = Ph (**9**), ^tBu (**10**)) are formed. **6**, **7**, **9**, and **10** slowly decompose on recrystallization from thf, Et_2O, or toluene with formation of $[\{(\eta\text{-}C_5H_4)_2CMe_2\}MCl_2]$ (M = Zr (**8**), Ti (**11**)). The formation of $(PR)_n$ (R = Ph, $n = 4-6$; R = ^tBu, $n = 4$) and PH_2R was shown by ^{31}P NMR spectroscopy. **2**, **4**, **5**−**8**, and **11** were characterized by NMR spectroscopy (^1H, ^{13}C, ^{31}P) and the paramagnetic Ti(III) complexes **9** and **10** by EPR spectroscopy and mass spectrometry. **5**, **8**, and **11** were also characterized by crystal structure determinations.

Introduction

After the discovery of α-olefin polymerization by Ziegler,[1] a vast number of metallocene and monocyclopentadienyl derivatives with different steric and electronic properties was prepared and employed as catalysts in polymerization reactions.

ansa-Metallocene dichlorides of Ti, Zr, and Hf (especially chiral ones; **A** in Figure 1) are important catalysts for the methylalumoxane (MAO)-promoted isotactic polymerization of olefins. Therefore, intensive research is being conducted toward synthesis of improved catalysts.[2−5]

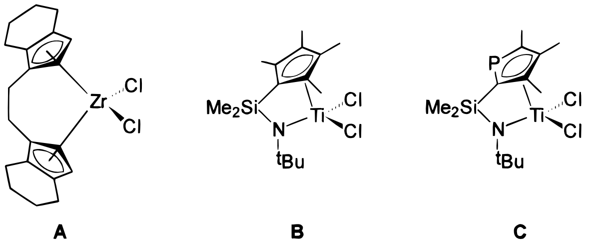

Figure 1. Selected examples of group 4 cyclopentadienyl complexes.

Recently, monocyclopentadienyl derivatives in which the cyclopentadienyl ring has a heteroatom-functionalized side chain (**B** in Figure 1), were prepared and employed in the polymerization of olefins and copolymerization of ethylene with propylene, 1-hexene, 1-octene or styrene.[6] These studies were also extended to phospholyl ligands (**C** in Figure 1).[7]

[†] Parts of this work were presented as a poster at the XVIII International Conference on Organometallic Chemistry, Munich, Germany, Aug 16−22, 1998; Abstract No. A223.

(1) Ziegler, K.; Holzkamp, E.; Breil, H.; Martin, H. *Angew. Chem.* **1955**, *67*, 541.

(2) Schneider, N.; Huttenloch, M. E.; Stehling, U.; Kirsten, R.; Schaper, F.; Brintzinger, H. H. *Organometallics* **1997**, *16*, 3413 and references therein.

(3) Kaminsky, W.; Rabe, O.; Schauwienold, A.-M.; Schupfner, G. U.; Hanss, J.; Kopf, J. *J. Organomet. Chem.* **1995**, *497*, 181.

(4) Chacon, S. T.; Coughlin, E. B.; Henling, L. M.; Bercaw, J. E. *J. Organomet. Chem.* **1995**, *497*, 171.

(5) (a) Kaminsky, W.; Külper, K.; Brintzinger, H. H.; Wild, F. R. W. P. *Angew. Chem.* **1985**, *97*, 507; *Angew. Chem., Int. Ed. Engl.* **1985**, *24*, 507. (b) Brintzinger, H. H.; Fischer, D.; Mülhaupt, R.; Rieger, B.; Waymouth, R. M. *Angew. Chem.* **1995**, *107*, 1255; *Angew. Chem., Int. Ed. Engl.* **1995**, *34*, 1143. (c) Fink, G.; Mülhaupt, R.; Brintzinger, H. *Ziegler Catalysts—Recent Scientific Innovations and Technological Improvements*; Springer-Verlag: Berlin, Heidelberg, New York, 1995.

(6) (a) Shapiro, P. J.; Bunel, E.; Schaefer, W. P.; Bercaw, J. E. *Organometallics* **1990**, *9*, 867. (b) Shapiro, P. J.; Cotter, W. D.; Schaefer, W. P.; Labinger, J. A.; Bercaw, J. E. *J. Am. Chem. Soc.* **1994**, *116*, 4623. (c) Flores, J. C.; Chien, J. C. W.; Rausch, M. D. *Organometallics* **1994**, *13*, 4140. (d) Alt, H. G.; Föttinger, K.; Milius, W. *J. Organomet. Chem.* **1999**, *572*, 21. (e) Galan-Fereres, M.; Koch, T.; Hey-Hawkins, E.; Eisen, M. *J. Organomet. Chem.* **1999**, *580*, 145. (f) McKnight, A. L.; Waymouth, R. M. *Chem. Rev.* **1998**, *98*, 2587. (g) Canich, J. A. M. Eur. Pat. 420 436, 1991. (h) Schmidt, G. F.; Timmers, F. J.; Knight, G. W.; Lai, S.-Y.; Nickias, P. N.; Rosen, R. K.; Stevens, J. C.; Wilson, D. R. Eur. Pat. 416 815, 1991.

10.1021/om990763z CCC: $19.00

While numerous O- and N-functionalized cyclopentadienyl ligands are known, the number of cyclopentadienes with a P-functionalized alkyl or silyl side chain is still small, and we have recently reported on the first compounds in which the P atom has a reactive phosphorus−substituent bond (e.g., P−H).[8,9] Such compounds should be useful precursors for dianionic bifunctional ligands in transition-metal chemistry. In addition, the presence of a P-containing group is advantageous for reactivity studies by ^{31}P NMR spectroscopy.[10]

We now report unexpected P−Si or P−C bond cleavage in the reactions of $Li_2[(C_5Me_4)SiMe_2PR]$ (R = cyclohexyl (Cy; **1**),[8] 2,4,6-$Me_3C_6H_2$ (Mes, **2**)) with $ZrCl_4$ and of $Li[(C_5H_4)CMe_2PHR]$ (R = Ph (**3**),[8] ^{t}Bu (**4**)) with $ZrCl_4$ or $[TiCl_3(thf)_3]$, which give the *ansa*-metallocenes $[\{(\eta\text{-}C_5Me_4)_2SiMe_2\}ZrCl_2]$ (**5**) and $[\{(\eta\text{-}C_5H_4)_2CMe_2\}MCl_2]$ (M = Zr (**8**), Ti (**11**)). **5**, **8**, and **11** were characterized by spectroscopy and by crystal structure determination. While the *ansa*-metallocene **5** has been reported before,[11] its structure was unknown up to now.

Results and Discussion

Synthesis. The general synthetic method for introduction of a cyclopentadienyl ligand into Zr or Ti complexes is salt elimination. We therefore prepared the (phosphanidosilyl)cyclopentadienides $Li_2[(C_5Me_4)SiMe_2PR]$ (R = Cy (**1**),[8] Mes (**2**)) from 1-$SiMe_2PHR$-2,3,4,5-Me_4C_5H and MeLi at −50 °C in thf. The neutral (phosphinosilyl)cyclopentadienes were obtained from (dimethylchlorosilyl)tetramethylcyclopentadiene and LiPHR at −80 °C followed by distillation. The (phosphinomethyl)cyclopentadienides $Li[(C_5H_4)CMe_2PHR]$ (R = Ph (**3**),[8] ^{t}Bu (**4**)) were obtained by the reaction of LiPHR with 6,6-dimethylfulvene in Et_2O.

After treating **1** and **2** with $ZrCl_4$ (ratio 1:1), we were, however, unable to isolate the expected cyclopentadienyl derivatives $[\{(\eta\text{-}C_5Me_4)SiMe_2PR\}MCl_2]$; instead, the *ansa*-metallocene $[\{(\eta\text{-}C_5Me_4)_2SiMe_2\}ZrCl_2]$ (**5**) was obtained after recrystallization from thf in good yield. The formation of $(PCy)_4$[12,13] or $(PHMes)_2$[14] in this reaction (eq 1) was shown by ^{31}P NMR spectroscopy. The Si compound which must have been formed could not be characterized by ^{29}Si NMR spectroscopy. These results are contrary to what was originally described by Dow Chemical Co. in a patent application. There, the reaction between the related dilithio salt $Li_2[(C_5Me_4)SiMe_2PPh]$ and $TiCl_4$ or $ZrCl_4$ was reported to give the expected products $[\{(\eta\text{-}C_5Me_4)SiMe_2PPh\}MCl_2]$, but no analytical or spectroscopic data were reported to support this assumption.[6h] **5** was previously prepared from $[ZrCl_4(thf)_2]$ and the dimetalated ligand in low yield (15%);[11] this is a general preparative method for *ansa*-metallocenes of Ti, Zr, and Hf.[2,3,4,11]

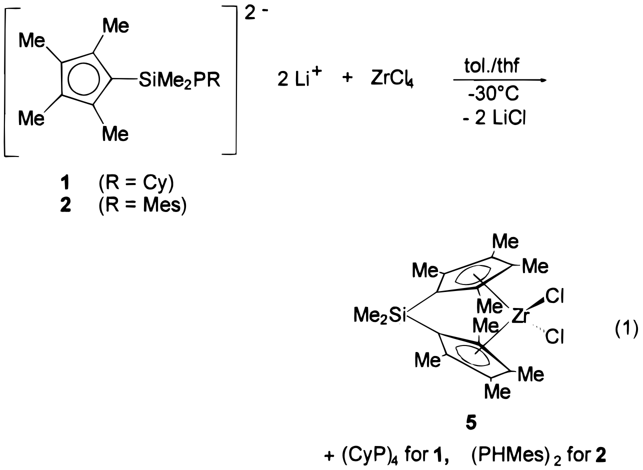

In the reaction of **3** or **4** with $ZrCl_4$ (Scheme 1) or $[TiCl_3(thf)_3]$ (Scheme 2), the formation of $[\{(\eta\text{-}C_5H_4)CMe_2PHR\}_2ZrCl_2]$ (R = Ph (**6**), ^{t}Bu (**7**)) as pale yellow solids and of $[\{(\eta\text{-}C_5H_4)CMe_2PHR\}_2TiCl]$ (R = Ph (**9**), ^{t}Bu (**10**)) as dark-green solids was observed. However, these compounds decompose slowly on recrystallization from thf, Et_2O, or toluene with formation of $[\{(\eta\text{-}C_5H_4)_2CMe_2\}MCl_2]$ (M = Zr (**8**), Ti (**11**)). The Ti compound that is presumably formed in addition to **11** could not be isolated. The decomposition is not influenced by light. The formation of cyclooligophosphanes $(PR)_n$[13] and PH_2R in this reaction was shown by ^{31}P NMR spectroscopy.

For **6**, the decomposition to **8** was studied in more detail. **6** was suspended in d_8-toluene (in which it is only slightly soluble), and d_8-thf was added until a clear solution had formed. The decomposition was studied by ^{1}H NMR spectroscopy. After 3 days at room temperature, the ratio of complexes **6** and **8** was 5:1, while at 50 °C, the ratio was 7:1 after 4 h. Complete formation of **8** from **6** had occurred after 8 days at room temperature. As the decomposition is spontaneous in methanol, **6** was dissolved in methanol, and the decomposition products were analyzed by GC-MS. Besides products which stem from a reaction with methanol, signals for phenylphosphine (*m*/*z* 110, high intensity), $PhP{=}CMe_2$ (*m*/*z* 150, medium intensity), and $(PPh)_4$ (*m*/*z* 429, medium intensity) were observed. While this experiment shows that neither propene nor polypropylene is formed, the mechanism of the formation of **5**, **8**, and **11** is still speculative.

The Ti(III) complexes **9** and **10** are highly air-sensitive. Brief exposure of toluene solutions to minute traces of oxygen apparently also triggers the quantitative formation of **11**.

A stable zirconocene derivative with [(diarylphosphino)isopropyl]cyclopentadienyl ligands, namely, $[\{(\eta\text{-}C_5H_4)CMe_2PR_2\}_2ZrCl_2]$ (R = *p*-tolyl, Ph), has been reported.[15]

The complexes **6**, **7**, **9**, and **10** were characterized by IR and ^{31}P NMR spectroscopy (the signals are only slightly broadened for **9** and **10**), **6** and **7** were also

---

(7) (a) Brown, S. J.; Gao, X.; Harrison, D. G.; Koch, L.; Spence, R. E. V. H.; Yap, G. P. A. *Organometallics* **1998**, *17*, 5445. (b) Mathey, F. *Chem. Rev.* **1998**, *88*, 429. (c) Janiak, C.; Lange, K. C. H.; Versteeg, U.; Lentz, D.; Budzelaar, P. *Chem. Ber.* **1996**, *129*, 1517. (d) Janiak, C.; Versteeg, U.; Lange, K. C. H.; Weimann, R.; Hahn, E. *J. Organomet. Chem.* **1995**, *501*, 219.

(8) Koch, T.; Hey-Hawkins, E. *Polyhedron* **1999**, *18*, 2113 and references therein.

(9) Slone, C. S.; Weinberger, D. A.; Mirkin, C. A. *Prog. Inorg. Chem.* **1999**, *48*, 233.

(10) Berger, S.; Braun, S.; Kalinowski, H. D. *NMR Spectroscopy*; Thieme Verlag: Stuttgart, Germany, 1993; Vol. 3 (^{31}P NMR Spectroscopy).

(11) Jutzi, P.; Dickbreder, R. *Chem. Ber.* **1986**, *119*, 1750.

(12) Bart, J. C. J. *Acta Crystallogr.* **1969**, *25B*, 762.

(13) Baudler, M.; Glinka, K. *Chem. Rev.* **1993**, *93*, 1623.

(14) Kurz, S.; Oesen, H.; Sieler, J.; Hey-Hawkins, E. *Phosphorus, Sulfur Silicon Relat. Elem.* **1996**, *117*, 189.

(15) Bosch, B. E.; Erker, G.; Fröhlich, R.; Meyer, O. *Organometallics* **1997**, *16*, 5449.

Scheme 1

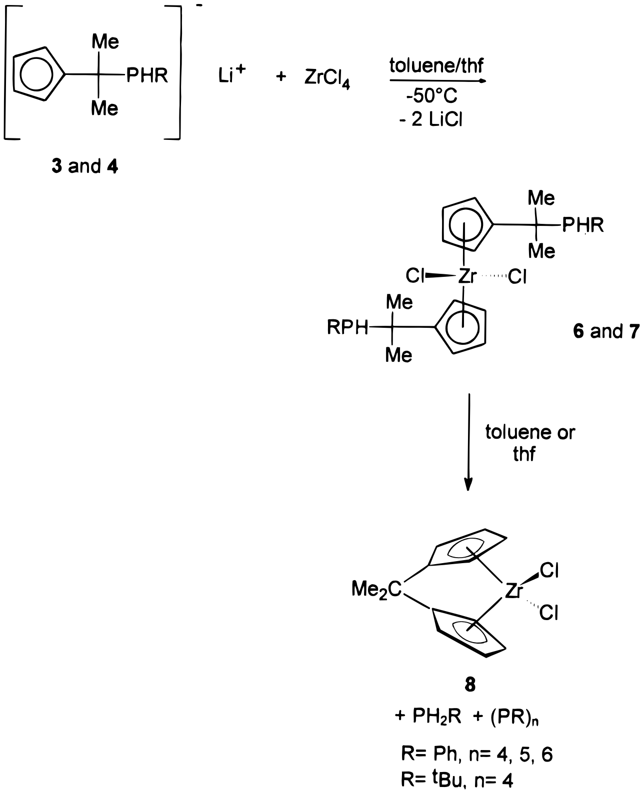

Scheme 2

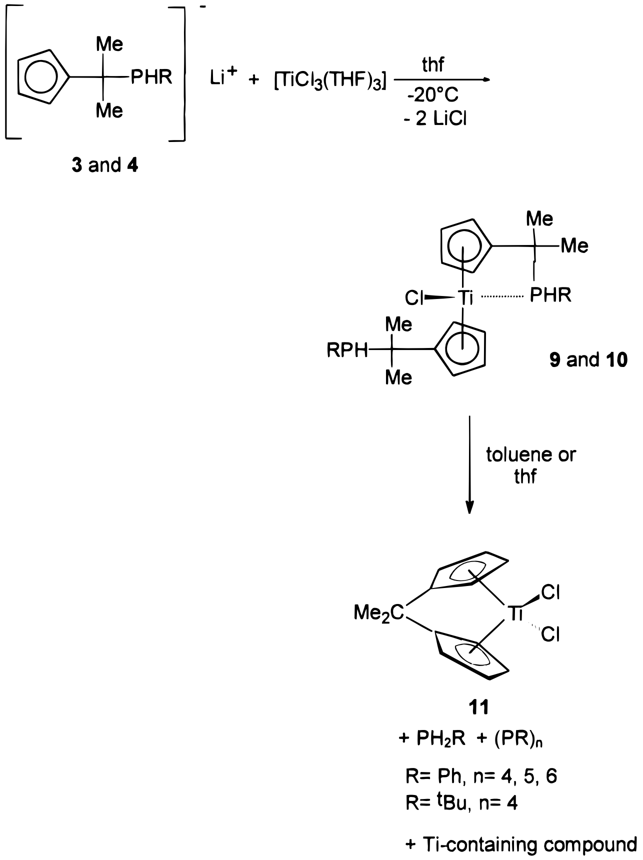

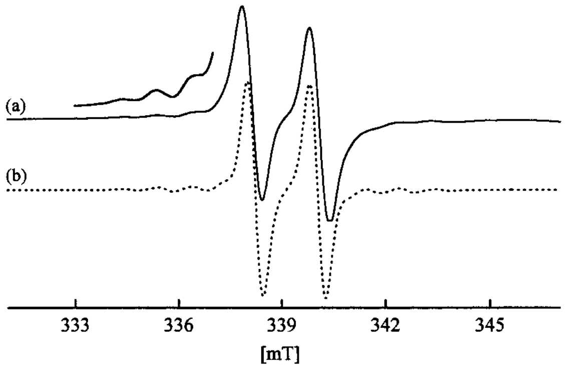

Figure 2. Experimental (a) and simulated (b) X-band EPR spectra of **10** in toluene at 295 K. The low-field part is additionally increased in intensity by a factor of 5.

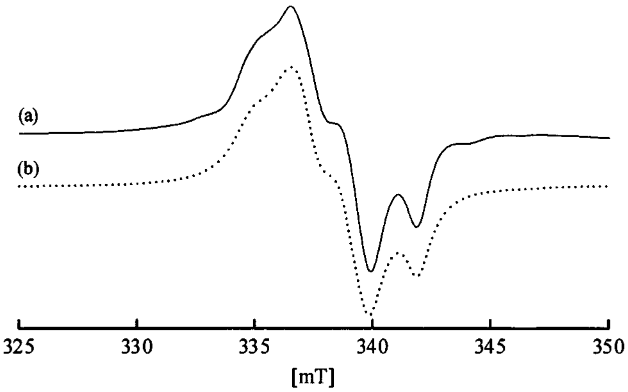

Figure 3. Experimental (a) and simulated (b) X-band EPR spectra of **10** in toluene at 130 K.

studied by ^{1}H NMR spectroscopy. The paramagnetic complexes **9** and **10** were also characterized by mass spectrometry and studied by EPR spectroscopy (vide infra). **6**, **7**, **9**, and **10** exhibit a doublet in the ^{31}P NMR spectrum (in C_6D_6), which is shifted to low field relative to **3** and **4** (**6**, 17.1 ppm ($^{1}J_{P-H} = 206.0$ Hz); **7**, 42.3 ppm ($^{1}J_{P-H} = 193.8$ Hz); **9**, 18.4 ppm (d, $^{1}J_{P-H} = 212.0$ Hz); **10**, 38.6 ppm (d, $^{1}J_{P-H} = 195.0$ Hz); **3**, −1.20 ppm (d of two q, $^{1}J_{P-H} = 207.5$ Hz, $^{3}J_{P-H} = 11.4$ Hz and $^{3}J_{P-H} = 15.8$ Hz);[8] **4**, −26.0 ppm (d of two dec, $^{1}J_{P-H} = 189.9$ Hz, $^{3}J_{P-H} = 11.0$ Hz)).

For **6** and **7**, molecular ion peaks were observed in the mass spectra, confirming their composition.

EPR Spectra of [{(η-C$_5$H$_4$)CMe$_2$PHR}$_2$TiCl] (R = Ph (9), ^{t}Bu (10)). For both Ti(III) complexes **9** and **10** intense EPR signals were observed. The room-temperature EPR spectrum of **10** is shown in Figure 2 together with its simulation. It consists of an intense doublet due to the interaction of the unpaired electron with one ^{31}P nucleus (nuclear spin $I = {}^{1}/_{2}$). Each of the doublet lines is symmetrically flanked by a hyperfine sextet resulting from the ^{47}Ti nucleus ($I = {}^{5}/_{2}$, natural abundance 7.4%) and a hyperfine octet caused by the ^{49}Ti nucleus ($I = {}^{7}/_{2}$, natural abundance 5.4%). Because of the similarity of the nuclear properties of the two Ti isotopes,[16] for each "^{31}P hyperfine line" an octet with the intensity ratio 0.7:1.9:1.9:1.9:1.9:1.9:1.9:0.7 was expected and observed. However, the intense "^{31}P doublet" prevents the observation of the "inner" lines (Figure 2) of the ^{47,49}Ti hyperfine pattern.

Figure 3 shows the EPR spectrum of **10** in a frozen solution ($T = 130$ K) together with its simulation. The spectrum is rhombic-symmetric, like that recorded for

---

(16) *BRUKER Almanac*; Bruker Analytic GmbH: Rheinstetten/Karlsruhe, Germany, 1999.

Table 1. EPR Parameters[a] for [{(η-C_5H_4)CMe_2PHPh}$_2$TiCl] (9)[b] and [{(η-C_5H_4)CMe_2PH^{t}Bu}$_2$TiCl] (10)[c]

tensor component	9	10	tensor component	9	10
g_1	2.006	2.007	A_1^P	14.5	14.8
g_2	1.990	1.992	A_2^P	15.2	15.4
g_3	1.975	1.975	A_3^P	18.4	18.9
g_{av}[d]	1.990	1.991	A_{av}^P[d]	16.0	16.4
g_0	1.989	1.990	a_0^P	16.3	16.9
a_0^{Ti}	9.8	9.6	solvent	thf	toluene

[a] Hyperfine coupling constants are given in 10^{-4} cm^{-1}. [b] g_i ±0.004; $A_i^{Ti,P}$ ±1.0. [c] g_i ±0.002; $A_i^{Ti,P}$ ±0.5. [d] $g_{av} = (g_1 + g_2 + g_3)/3$; $A_{av}^P = (A_1^P + A_2^P + A_3^P)/3$.

9. All spectra can be described with the spin Hamiltonian (2), with $S = {}^1/_2$; all other symbols have their usual meaning.

$$\mathbf{H}_{sp} = \mathbf{g}\cdot\mu_B\cdot\mathbf{S}\cdot\mathbf{B}_0 + \mathbf{S}\cdot\mathbf{A}^P\cdot\mathbf{I}^P + \mathbf{S}\cdot\mathbf{A}^{Ti}\cdot\mathbf{I}^{Ti} \qquad (2)$$

In Table 1 the principal values obtained for the **g** tensor and the ^{31}P and ^{47,49}Ti hyperfine structure (=hfs) tensors $\mathbf{A}^P$ and $\mathbf{A}^{Ti}$ are listed. Anisotropic ^{47,49}Ti hfs couplings were observed in the frozen-solution spectra, but unfortunately they could not be analyzed in detail because (i) the line widths of the frozen-solution spectra are 2.5 times larger than those observed in liquid solution, (ii) the intensity of the Ti satellite lines is low (<2% of the major signals), and (iii) the small **g** tensor anisotropy results in excessive line overlap, which prevents an unambiguous analysis of the observed ^{47,49}Ti satellites. In addition, ^{47,49}Ti hfs coupling parameters so far observed[17] are small and lie only in the range of (10−20) × 10^{-4} cm^{-1}. In our case (compound **10**) a maximum Ti hfs coupling constant of about 18 × 10^{-4} cm^{-1} can be estimated, which we ascribe to A_z^{Ti}.

The hfs parameters can be used to estimate the spin density on the nuclei and, therefore, allow conclusions to be made about the nature of the M−L bonds, in particular the hybridization of the orbitals.[18,19] For this, the complete parameters of the hfs tensors are needed. The spin densities $(c_{s,p,d}^X)^2$ can then be obtained by using eqs 3a,b, where s, p, and d represent atomic

$$(c_s^X)^2 = a_{av,exptl}^X / a_{av,theor}^X \qquad (3a)$$

$$(c_{p,d}^X)^2 = b_{exptl}^X / b_{theor}^X \qquad (3b)$$

orbitals, X is the nucleus under discussion, a_{av}^X is the isotropic hyperfine coupling constant, and b^X is the dipolar part of the hyperfine tensors. For the ^{31}P nucleus the complete tensor has been obtained. Using the values for the parameters $a_{av,theor}^X$ and b_{theor}^X calculated by Morton and Preston[19] and eqs 3a,b gave the following spin densities for the ^{31}P 3s and 3p orbitals: $(c_s^P)^2$ = 0.004 and $(c_p^P)^2$ = 0.010. The latter values can be used to estimate the 3s/3p hybridization of the P atom (eq 4), where α_P^2 is the overall spin density on the P atom and amounts to α_P^2 = 1.4%.

$$(c_s^P)^2 = \alpha_P^2(1 - n^2) \qquad (c_p^P)^2 = \alpha_P^2 n^2 \qquad (4)$$

For the degree of hybridization n^2 a value of 0.71 was obtained, which is close to that expected for a distorted tetrahedrally coordinated P atom. This corresponds to the structure proposed for the Ti(III) complex under study.

To our knowledge, up to now, ^{31}P hfs interactions were only observed for the Ti(III) complex [Cp_2TiMe(PPh_3)].[20] The observed isotropic ^{31}P hfs coupling constant of $a_0^P = 17.6 \times 10^{-4}$ cm^{-1} is close to those obtained by us. Unfortunately, no anisotropic ^{31}P hfs data were reported,[20] so that no conclusions can be drawn about the overall spin density and the degree of hybridization n^2 on the P atom.

Similar properties were observed by Xin et al. for [(Cp_2Ti)$_2$(μ-H)(μ-PCy_2)].[21] This Ti(III) complex exhibits no EPR signal at 253 K; this indicates the presence of diamagnetic species. At room temperature, the EPR spectrum shows an intense singlet (g_0 = 1.9808, a_0^{Ti} = 9.43 G). No ^{31}P hfs interaction was observed.

Because of the lack of a complete parameter set for the ^{47,49}Ti hyperfine tensor $\mathbf{A}^{Ti}$, only a rough estimate of the spin density on the metal atom can be made. From the isotropic Ti hfs coupling and by using eq 3a and $a_{av,theor}^{Ti} = 260.8 \times 10^{-4}$ cm^{-1},[19] a Ti 4s contribution of 3.7% can be calculated. To estimate the Ti 3d contribution, we assume the observed maximum Ti hfs coupling constant of about 18 × 10^{-4} cm^{-1} as being the axial component A_z^{Ti} of the Ti hfs tensor. Then, from $A_z^{Ti} - a_0^{Ti} = 2b$, a b value of 4.2 × 10^{-4} cm^{-1} was obtained. With $b_{theor}^X = 7 \times 10^{-4}$ cm^{-1},[19] eq 3 yields a Ti 3d contribution of about 60%. Therefore, roughly 65% of the unpaired spin density is located on the metal. Since the spin density determined for the coordinating P atom is small, the residual spin density is expected to be located on the Cl and Cp ligands.

Molecular Structures of [{(η-C_5Me_4)$_2$$SiMe_2$}$ZrCl_2$] (5) and [{($\eta$-$C_5H_4$)$_2$$CMe_2$}$MCl_2$] (M = Zr (8), Ti (11)). Compound **5** was obtained as pale green crystals from thf and crystallizes in the monoclinic space group *C*2/*c* (Figure 4). Complex **8** was obtained as yellow crystals on recrystallizing **6** or **7** from thf after several days. Accordingly, **11** is obtained on recrystallizing **9** or **10** from thf after several days as dark red crystals. **8** (Figure 5) and **11** (Figure 6) are isotypic and isostructural and crystallize in the monoclinic space group $P2_1/m$.

In **5**, the Zr atom and the Si atom of the $SiMe_2$ bridge are located on a crystallographic C_2 axis which generates the atoms "a". In **8** and **11**, the metal atom (Zr or Ti) as well as Cl(1), Cl(2), and the C atoms of the CMe_2 bridge (C(1), C(2), C(3)) are located on a crystallographic mirror plane, by which the atoms "a" are generated. A comparison of **5**, **8**, and **11** with related *ansa*-metallocenes is given in Tables 2 and 3, respectively. The Zr−Cl and Si−C bond lengths of **5** are in the range observed for related complexes (Table 2). The Zr−CEN distance

---

(17) Bajgur, C. S.; Tikkanen, W. R.; Petersen, J. L. *Inorg. Chem.* **1985**, *24*, 2539.

(18) Kirmse, R.; Stach, J. *ESR-Spektroskopie-Anwendungen in der Chemie*; Akademie-Verlag: Berlin, 1985; pp 86−95.

(19) Morton, J. R.; Preston, K. F. *J. Magn. Reson.* **1978**, *30*, 577.

(20) Klei, E.; Teuben, J. H. *J. Organomet. Chem.* **1980**, *188*, 97.

(21) Xin, S.; Woo, H. G.; Harrod, J. F.; Samuel, E.; Lebuis, A. *J. Am. Chem. Soc.* **1997**, *119*, 5307.

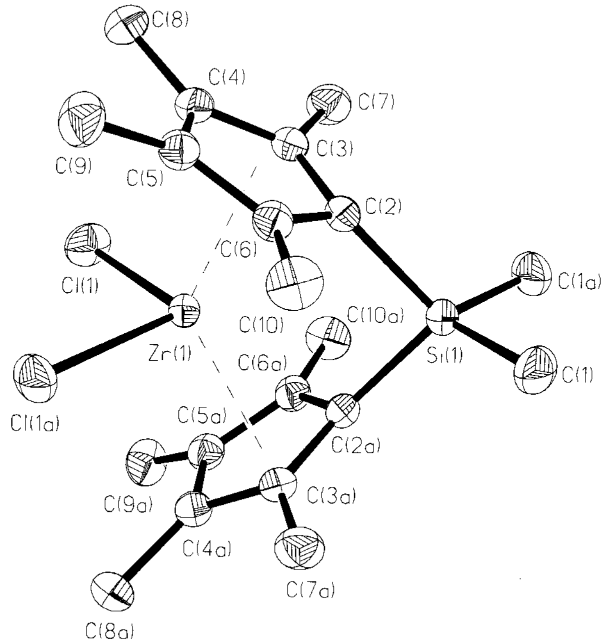

Figure 4. Molecular structure of $[\{(\eta\text{-}C_5Me_4)_2SiMe_2\}ZrCl_2]$ (**5**) showing the atom-numbering scheme employed (ORTEP plot, 50% probability, SHELXTL PLUS; XP[32]). Hydrogen atoms are omitted for clarity.

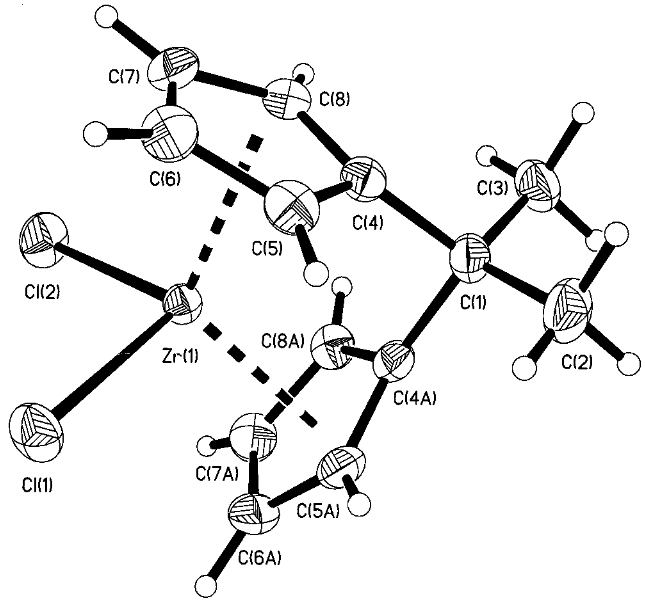

Figure 5. Molecular structure of $[\{(\eta\text{-}C_5H_4)_2CMe_2\}ZrCl_2]$ (**8**) showing the atom-numbering scheme employed (ORTEP plot, 50% probability, SHELXTL PLUS; XP[32]). Hydrogen atoms are omitted for clarity.

is about 0.1 Å larger. As no data for the $CMe_2-C(Cp)$ bond lengths are given in the literature, the bond lengths of C(1)−C(4) and C(1)−C(4A) of 1.532(3) Å in **8** and **11** cannot be compared with known values (Table 3). Of the reported complexes, **8** has the smallest CEN−Zr−CEN bite angle (116.7°).

Experimental Section

All experiments were carried out under purified dry argon. Solvents were dried and freshly distilled under argon. The NMR spectra were recorded at 25 °C in C_6D_6 with an AVANCE DRX 400 spectrometer (Bruker), ^1H NMR: internal standard, solvent (benzene); external standard, TMS. ^{13}C NMR: external standard, TMS; internal standard, solvent. ^{31}P NMR: external standard, 85% H_3PO_4. The IR spectra were recorded on a FT-IR spectrometer Perkin-Elmer System 2000 in the range 350−4000 cm^{-1}. GC-MS: Hewlett-Packard HP 6890 GC, HP 5973 MSD (mass selective detector). EPR spectra were recorded in the X-band ($\nu \approx 9.5$ GHz) with a Bruker ESP 300E spectrometer in the temperature range 295 K $\geq T \geq$ 130 K by using about 10^{-3} M solutions of **9** (thf) and **10** (toluene). The EPR parameters were obtained by using the computer program Win-EPR-SimFonia.[28] The melting points were determined in sealed capillaries under argon and are uncorrected. $Li_2[(C_5Me_4)SiMe_2PCy]$ (**1**),[8] $Li[(C_5H_4)CMe_2PHPh]$ (**3**),[8] $[TiCl_3(thf)_3]$,[29] and 1-SiMe$_2$Cl-2,3,4,5-Me$_4$C$_5$H[30] were prepared according to the literature procedures. $ZrCl_4$ is commercially available.

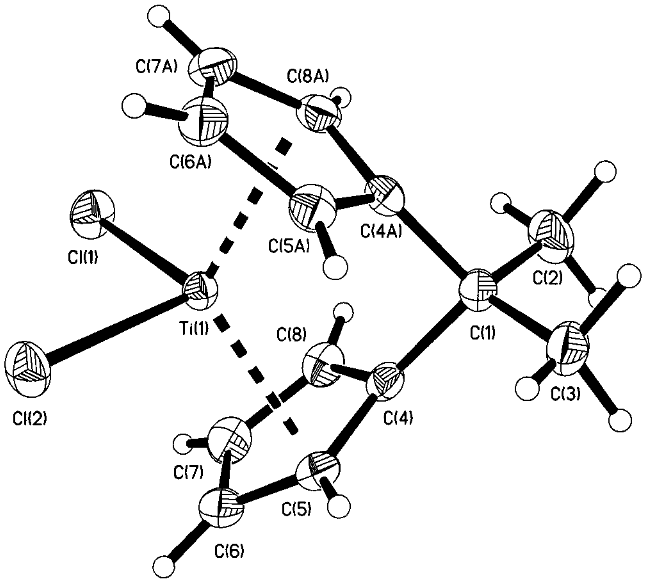

Figure 6. Molecular structure of $[\{(\eta\text{-}C_5H_4)_2CMe_2\}TiCl_2]$ (**11**) showing the atom-numbering scheme employed (ORTEP plot, 50% probability, SHELXTL PLUS; XP[32]). Hydrogen atoms are omitted for clarity.

Synthesis of 1-SiMe$_2$PHMes-2,3,4,5-Me$_4$C$_5$H (2a). LiPHMes (3.50 g, 22.2 mmol) was suspended in a mixture of *n*-hexane (50 mL) and Et_2O (5 mL) and cooled to −80 °C. (Dimethylchlorosilyl)tetramethylcyclopentadiene (4.83 g, 22.5 mmol) was added, and the reaction mixture was warmed to ambient temperature. The mixture was stirred for 3 days, after which the yellow color of the lithium phosphanide had disappeared completely. The mixture was filtered, the solvent evaporated in vacuo, and the resulting yellow oil distilled under reduced pressure (100−115 °C, $2 \cdot 10^{-3}$ Torr), giving 2.2 g (30%) of **2a** as a yellow oil. ^1H NMR (C_6D_6): δ 6.76 (s, 2H, *m*-H in Mes), 3.30 (d, 1H, PH, $^1J_{P-H} = 211.4$ Hz), 2.86 (s, 1H, C$_5$*H*Me$_4$), 2.33 (s, 6H, *o*-CH$_3$ in Mes), 2.10 (s, 3H, *p*-CH$_3$ in

---

(22) Herrmann, W. A.; Rohrmann, J.; Herdtweck, E.; Spaleck, W.; Winter, A. *Angew. Chem.* **1989**, *101*, 1536; *Angew. Chem., Int. Ed. Engl.* **1989**, *28*, 1511.

(23) Spaleck, W.; Antberg, M.; Rohrmann, J.; Winter, A.; Bachmann, B.; Kiprof, P.; Behm, J.; Herrmann, W. A. *Angew. Chem.* **1992**, *104*, 1371; *Angew. Chem., Int. Ed. Engl.* **1992**, *31*, 1345.

(24) Razavi, A.; Atwood, J. L. *J. Organomet. Chem.* **1995**, *497*, 105.

(25) Willoughby, C. A.; Davis, W. M.; Buchwald, S. L. *J. Organomet. Chem.* **1995**, *497*, 11.

(26) Smith, J. A.; von Seyerl, J.; Huttner, G.; Brintzinger, H. H. *J. Organomet. Chem.* **1979**, *173*, 175.

(27) Nifant'ev, I. E.; Churakov, A. V.; Urazowski, I. F.; Mkoyan, Sh. G.; Atovmyan, L. O. *J. Organomet. Chem.* **1992**, *435*, 37.

(28) Weber, R. T. WIN-EPR-SimFonia, Version 1.2; EPR Division, Bruker Instruments Inc., 1995.

(29) Manzer, L. F. *Inorg. Synth.* **1982**, *21*, 135.

(30) Plenio, H. *Chem. Ber.* **1991**, *124*, 2185.

Table 2. Comparison of Selected Bond Lengths (Å) and Angles (deg) of 5 with Those of Related Silylene-Bridged Zirconocene Dichloride Complexes

compd	Zr−C	Si−C(Cp)	Zr−CEN	Cl−Zr−Cl	CEN−Zr−CEN[a]	C(Cp)−Si−C(Cp)	ref
rac-[{(2-methyltetrahydrobenz[*e*]indenyl)$_2$-SiMe$_2$}ZrCl$_2$]	2.4100(7)	1.876(3)	2.238	97.35(4)	128.1	95.6(2)	2
rac-[({bis(4,5,6,7-tetrahydroindenyl)}SiMe$_2$)ZrCl$_2$]	2.444, 2.440	*b*	2.226, 2.225	97.3	126.3	*b*	3
[({bis(2,4,7-trimethylindenyl)}SiMe$_2$)ZrCl$_2$]	2.414, 2.414	*b*	2.236, 2.236	97.2	129.5	*b*	3
rac-[{(2-SiMe$_3$-4-Bu^t-C$_5$H$_2$)$_2$SiMe$_2$}ZrCl$_2$]	2.435(1), 2.422(1)	1.872(3), 1.879(3)	2.233, 2.233	97.6(3)	126.7	94.0(1)	4
[{(η-C$_5$H$_4$)$_2$SiMe$_2$}ZrCl$_2$]	2.435(1)	1.866(4)	2.197	97.98(4)	125.4	93.2(2)	17
rac-[({bis(indenyl)}SiMe$_2$)ZrCl$_2$]	2.431(1)	1.871(1)	2.293	98.76(1)	119.0	94.57(6)	22
rac-[({bis(2-methylindenyl)SiMe$_2$})ZrCl$_2$]	2.419	*b*	2.244	99.06	128.1	94.3(1)	23
[{(η-C$_5$Me$_4$)$_2$SiMe$_2$}ZrCl$_2$] (**5**)	2.4334(7)	1.887(2)	2.329	99.28(3)	128.6	95.7(1)	this work

[a] CEN = center of the cyclopentadienyl ring. [b] No value given.

Table 3. Comparison of Selected Bond Lengths (Å) and Angles (deg) of 8 and 11 with Those of Related Methylene-Bridged Titanocene and Zirconocene Dichloride (and Dimethyl) Complexes

compd	M−Cl	C$_{br}$−C(Cp)	M−CEN	Cl−M−Cl	CEN−M−CEN[a]	C(Cp)−C−C(Cp)	ref
[Me$_2$C{(3-Bu^t-C$_5$H$_3$)-9-fluorenyl}ZrCl$_2$]	2.420, 2.420	*b*	2.184, 2.245	96.2	118.5	*b*	3
[Me$_2$C{(3-Me-C$_5$H$_3$)−9-fluorenyl}ZrCl$_2$]	2.425(3), 2.403(3)	*b*	2.16, 2.26	99.1	118.6	98.4	24
[cyclo-C$_6$H$_{10}$(η-C$_5$H$_4$)(4,5,6,7-tetrahydro-indenyl)})TiCl$_2$]	2.346(2), 2.338(2)	*b*	2.07, 2.08	97.6(1)	121.8	96.3(4)	25
[{(η-C$_5$H$_4$)$_2$CH$_2$}TiCl$_2$]	2.33(1), 2.34(1)	1.53(5)	2.05, 206	97.2(3)	121	99(2)	26
[{(η-C$_5$H$_4$)$_2$CMe$_2$}TiMe$_2$]		1.465(6)	*b*		120.9	*b*	27
[{(η-C$_5$H$_4$)$_2$CMe$_2$}ZrMe$_2$]		1.441(6)	*b*		115.9	*b*	27
[{(η-C$_5$H$_4$)$_2$CMe$_2$}ZrCl$_2$] (**8**)	2.4321(8), 2.4406(8)	1.532(3)	2.213	100.25(3)	116.7	99.5(2)	this work
[{(η-C$_5$H$_4$)$_2$CMe$_2$}TiCl$_2$] (**11**)	2.333(1), 2.352(1)	1.532(3)	2.193	98.04(4)	121.6	96.6(2)	this work

[a] CEN = center of the cyclopentadienyl ring. [b] No value given.

Mes), 1.97 (s, 6H, CH$_3$ in C$_5$Me$_4$), 1.84 (s, 6H, CH$_3$ in C$_5$Me$_4$), 0.17 (d, 6H, SiMe$_2$, $^3J_{P-H}$ = 5.0 Hz). ^{31}P NMR (C$_6$D$_6$): δ −168.6 (d, $^1J_{P-H}$ = 212.0 Hz). EI-MS: *m/z* 328 (25) [M$^+$], 179 (100) [(CH$_3$)$_4$C$_5$Si(CH$_3$)$_2$$^+$], 151 (85) [PHMes$^+$], and fragmentation thereof. Anal. Calcd for C$_{20}$H$_{31}$SiP (328.51): C, 72.7; H, 9.4; P, 9.4. Found: C, 67.3 (lower due to silicon carbide formation); H, 9.0; P, 9.2.

Synthesis of Li$_2$[(C$_5$Me$_4$)SiMe$_2$PMes] (2). 2a (2.2 g, 6.7 mmol) was dissolved in thf (50 mL), and at −50 °C an MeLi solution (8.9 mL of a 1.5 M solution in Et$_2$O) was added slowly. The mixture was then brought to ambient temperature and refluxed for 5 h. The compound was used without further purification. ^{31}P NMR (thf/ C$_6$D$_6$): δ −181.2 br, s.

Synthesis of Li[(C$_5$H$_4$)CMe$_2$PH^{t}Bu] (4). 6,6-Dimethylfulvene (1.34 g, 12.6 mmol) was added to a suspension of LiPH^{t}Bu (1.21 g, 12.6 mmol) in Et$_2$O (30 mL), and the reaction mixture was stirred for 12 h. The resulting solid was isolated by filtration and washed twice with *n*-hexane to yield **4** as a pale yellow powder (1.5 g, 58%). Mp: 120 °C dec. ^{1}H NMR (thf-d_8): δ 6.06 (s, 2H, C*H* in C$_5$H$_4$), 6.00 (s, 2H, C*H* in C$_5$H$_4$), 3.57 (d, 1H, P−H, $^1J_{P-H}$ = 199.2 Hz), 1.82 (d, 3H, C(CH$_3$)$_2$, $^3J_{P-H}$ = 14.2 Hz), 1.80 (d, 3H, C(CH$_3$)$_2$, $^3J_{P-H}$ = 14.3 Hz), 1.16 (d, 9H, C(CH$_3$)$_3$, $^3J_{P-H}$ = 10.6 Hz). ^{13}C NMR (thf-d_8): δ 132.23 (d, *ipso*-C in C$_5$H$_4$, $^2J_{P-C}$ = 8.5 Hz), 103.39 (C3, C4 in C$_5$H$_4$), 102.46 (d, C2, C5 in C$_5$H$_4$, $^3J_{P-C}$ = 3.3 Hz), 39.53 (d, C−*C*H$_3$, $^2J_{P-C}$ = 10.3 Hz), 35.33 (d, *C*(CH$_3$)$_2$, $^1J_{P-C}$ = 15.6 Hz), 34.08 (d, *C*(CH$_3$)$_3$, $^1J_{P-C}$ = 15.1 Hz), 33.52 (d, C−*C*H$_3$, $^2J_{P-C}$ = 11.7 Hz), 31.89 (d, C(*C*H$_3$)$_3$, $^2J_{P-C}$ = 12.7 Hz). ^{31}P NMR (thf, C$_6$D$_6$): δ 26.0 (d of two dec, $^1J_{P-H}$ = 189.9 Hz, $^3J_{P-H}$ = 11.0 Hz). ^{7}Li NMR (thf-d_8): δ −4.6, s. IR (KBr): ν (cm^{-1}): 2282 m (ν(PH)), 1606 br, m (Cp, ν(C=C)). Anal. Calcd for C$_{12}$H$_{20}$PLi (202.20): C, 71.3; H, 10.0; P, 15.3. Found: C, 70.9; H, 9.8; P, 15.9. Recrystallization from Et$_2$O gave colorless crystals.

Synthesis of *ansa*-{Dimethylsilylbis(tetramethylcyclopentadienyl)}zirconium Dichloride (5). (a) From ZrCl$_4$ and Li$_2$[(C$_5$Me$_4$)SiMe$_2$PCy] (1). A 0.76 g (3.3 mmol) amount of ZrCl$_4$ was suspended in 30 mL of toluene, and a solution of 1.00 g (3.3 mmol) of Li$_2$[(C$_5$Me$_4$)SiMe$_2$PCy] (**1**) in 25 mL of thf was added dropwise at −30 °C. The solution turned dark red immediately. The reaction mixture was stirred at room temperature for 12 h. Then the solvent was removed in vacuo and the residue washed with 20 mL of pentane. The resulting yellow powder was recrystallized from thf, yielding 0.72 g of **5** (82% relative to **1**) as pale green crystals. The product (PCy)$_4$[13] (^{31}P NMR (C$_6$D$_6$): δ −68.4 s) was detected by ^{1}H and ^{31}P NMR spectroscopy.

(b) From ZrCl$_4$ and Li$_2$[(C$_5$Me$_4$)SiMe$_2$PMes] (2). Alternatively, **5** was obtained from ZrCl$_4$ (1.00 g, 4.4 mmol) in 30 mL of toluene and Li$_2$[(C$_5$Me$_4$)SiMe$_2$PMes] (**2**; 1.50 g, 4.4 mmol) in 25 mL of thf at −30 °C. Yield: 1.41 g (70% relative to **2**). The product (PHMes)$_2$[14] (^{31}P NMR (C$_6$D$_6$): δ −111.1, *meso* isomer; −118.5, *d* and *l* isomer) was detected by ^{1}H and ^{31}P NMR spectroscopy.

^{1}H and ^{13}C NMR (in CDCl$_3$) are in agreement with the literature values.[11] In C$_6$D$_6$, the signals are shifted slightly: ^{1}H NMR δ 2.07 (s, 12H, C$_5$*Me*$_4$), 1.79 (s, 12H, C$_5$*Me*$_4$), 0.61 (s, 6H, Si*Me*$_2$).

Synthesis of *ansa*-{Dimethylmethanylbis(cyclopentadienyl)}zirconium Dichloride (8). (a) From ZrCl$_4$ and Li[(C$_5$H$_4$)CMe$_2$PHPh] (3). A 1.30 g (5.6 mmol) amount of ZrCl$_4$ was suspended in 50 mL of toluene, and a solution of 1.24 g (5.6 mmol) of Li[(C$_5$H$_4$)CMe$_2$PHPh] (**3**) in 20 mL of thf was added dropwise at −50 °C. The solution turned dark red immediately. The reaction mixture was stirred at room temperature for 12 h. Then the solvent was removed in vacuo and the residue washed with 50 mL of pentane. The resulting pale yellow powder exhibits a doublet in the ^{31}P NMR spectrum (C$_6$D$_6$) at 17.1 ppm ($^1J_{P-H}$ = 206.0 Hz), which is consistent with the presence of the complex [{(η-C$_5$H$_4$)CMe$_2$PHPh}$_2$ZrCl$_2$] (**6**). On recrystallization from thf, **6** decomposed over several days with formation of **8**. Yield: 1.17 g of **8** (61% relative to **3**) as yellow crystals. The products (PPh)$_n$[13] (n = 4−6) and PH$_2$Ph were detected by ^{31}P NMR spectroscopy (C$_6$D$_6$: δ −4.0 (m, (PPh)$_5$), −26.4 (s, (PPh)$_6$), −47.7 (s, (PPh)$_4$), −123.8 (t, PH$_2$-Ph, $^1J_{P-H}$ = 197 Hz)).

(b) From ZrCl$_4$ and Li[(C$_5$H$_4$)CMe$_2$PH^{t}Bu] (4). Alternatively, **8** was obtained from ZrCl$_4$ (1.10 g, 4.7 mmol) in 50 mL of toluene and Li[(C$_5$H$_4$)CMe$_2$PH^{t}Bu] (**4**; 0.95 g, 4.7 mmol) in 20 mL of Et$_2$O at −50 °C. The solution turned dark red immediately. The reaction mixture was stirred at room temperature for 24 h. Then the solvent was removed in vacuo and the residue washed with 25 mL of pentane. The resulting pale yellow powder exhibits a doublet in the ^{31}P NMR spectrum (C_6D_6) at 42.3 ppm ($^1J_{P-H} = 193.8$ Hz), consistent with the presence of the complex [{(η-C_5H_4)CMe_2PH^tBu}$_2$$ZrCl_2$] (**7**). On recrystallization from thf, **7** slowly decomposed over several days with formation of **8**. Yield: 1.2 g of **8** (75% relative to **4**) as yellow crystals. The products (P^tBu)$_4$[13] and $PH_2{}^tBu$ were detected by ^{31}P NMR spectroscopy (C_6D_6: δ −32.4 (s, ?), −59.0 (s, (P^tBu)$_4$), −80.1 (t, $PH_2{}^tBu$, $^1J_{P-H} = 174$ Hz)).

[{(η-C_5H_4)CMe_2PHPh}$_2$$ZrCl_2$] (6). ^{1}H NMR (thf-$d_8$): δ 7.36 (m, 2H, Ph), 7.28 (m, 2H, Ph), 7.10−6.93 (m, 6H, Ph), 6.03 (m, 1H, C*H* in C_5H_4), 5.99 (t, 1H, C*H* in C_5H_4, $^3J_{H-H} = 2.7$ Hz), 5.95 (t, 1H, C*H* in C_5H_4, $^3J_{H-H} = 2.7$ Hz), 5.88 (t, 1H, C*H* in C_5H_4, $^3J_{H-H} = 2.7$ Hz), 5.85 (m, 1H, C*H* in C_5H_4, $^3J_{H-H} = 3.5$ Hz), 5.79 (m, 1H, C*H* in C_5H_4), 5.77 (m, 1H, C*H* in C_5H_4), 5.73 (m, 1H, C*H* in C_5H_4), 4.00 (d, 2H, P−H, $^1J_{P-H} = 207.3$ Hz), 1.11 (d, 6H, CH_3, $^3J_{H-H} = 9.8$ Hz), 1.10 (d, 6H, CH_3, $^3J_{H-H} = 9.8$ Hz). ^{31}P NMR (C_6D_6): δ 17.1 (d, $^1J_{P-H} = 206.0$ Hz). IR (KBr): ν (cm^{-1}): 2292 m (ν(PH)).

[{(η-C_5H_4)CMe_2PH^tBu}$_2$$ZrCl_2$] (7). ^{1}H NMR ($C_6D_6$): δ 6.26 (t, 4H, C*H* in C_5H_4, $^3J_{H-H} = 2.8$ Hz), 6.01 (m, 4H, C*H* in C_5H_4), 3.57 (d, 2H, P−H, $^1J_{P-H} = 189.0$ Hz), 1.75 (m, 6H, CH_3 in CMe_2) 1.71 (m, 6H, CH_3 in CMe_2), 0.86 (d, 18H, CH_3 in ^{t}Bu, $^3J_{P-H} = 11.4$ Hz). ^{31}P NMR (C_6D_6): δ 42.3 (d, $^1J_{P-H} = 193.8$ Hz). IR (KBr): ν (cm^{-1}): 2379 m (ν(PH)).

[{(η-C_5H_4)$_2$$CMe_2$}$ZrCl_2$] (8). ^{1}H NMR ($C_6D_6$): δ 6.38 (t, 4H, C*H* in C_5H_4, $^3J_{H-H} = 2.7$ Hz), 5.15 (t, 4H, C*H* in C_5H_4, $^3J_{H-H} = 2.7$ Hz), 1.07 (s, 6H, CH_3). ^{13}C NMR (C_6D_6): δ 123.23 (s, 4C, C_5H_4), 123.05 (s, 2C, *ipso*-C in C_5H_4), 107.17 (s, 4C, C_5H_4), 37.92 (s, 1C, *C*−CH_3), 24.10 (s, 2C, CH_3). EI-MS: 332 (100) [M$^+$], 296 (25) [M$^+$ − Cl], 281 (25) [M$^+$ − Cl − Me]. Anal. Calcd for $C_{13}H_{14}ZrCl_2$ (332.38): C, 47.0; H, 4.2. Found: C, 46.7; H, 4.1.

Synthesis of *ansa*-{Dimethylmethanylbis(cyclopentadienyl)}titanium Dichloride (11). (a) From [$TiCl_3(thf)_3$] and Li[(C_5H_4)CMe_2PHPh] (3). A 1.25 g (3.4 mmol) amount of [$TiCl_3(thf)_3$] was dissolved in 25 mL of thf, and a solution of 0.75 g (3.4 mmol) of Li[(C_5H_4)CMe_2PHPh] (**3**) in 30 mL of thf was added at −20 °C. The solution turned dark green immediately. The reaction mixture was stirred at room temperature for 12 h. Then the solvent was removed in vacuo and the residue washed with 20 mL of hexane. The resulting green powder (complex **9**) was recrystallized from thf. The EPR spectrum of this highly air-sensitive solution showed the presence of a paramagnetic Ti(III) species ([{(η-C_5H_4)CMe_2PHPh}$_2$TiCl] (**9**)) which exhibits Ti−P interaction. The ^{31}P NMR spectrum (C_6D_6) showed a doublet at 18.4 ppm ($^1J_{P-H} = 212.0$ Hz). The dark green solution decomposes slowly over several days with formation of a red solution from which dark red crystals of **11** can be obtained. Yield: 0.54 g (55% relative to **3**). The products $(PPh)_n$[13] (n = 4−6) and PH_2Ph were detected by ^{31}P NMR spectroscopy (C_6D_6: δ −4.0 (m, $(PPh)_5$), −26.4 (s, $(PPh)_6$), −47.7 (s, $(PPh)_4$), −123.8 (t, PH_2Ph, $^1J_{P-H} = 197$ Hz)).

(b) From [$TiCl_3(thf)_3$] and Li[(C_5H_4)CMe_2PH^tBu] (4). Alternatively, **11** was obtained from 1.00 g (2.7 mmol) of [$TiCl_3(thf)_3$], dissolved in 25 mL of thf and a solution of 0.60 g (2.7 mmol) of Li[(C_5H_4)CMe_2PH^tBu] (**4**) in 30 mL of thf at −20 °C. The solution turned dark green immediately. The reaction mixture was stirred at room temperature for 12 h. Then the solvent was removed in vacuo and the residue washed with 20 mL of hexane.The resulting green powder (complex **10**) was recrystallized from toluene. An EPR spectrum of this highly air-sensitive solution showed the presence of a paramagnetic Ti(III) species ([{(η-C_5H_4)CMe_2PH^tBu}$_2$TiCl] (**10**)) which exhibits Ti−P interaction. The dark green solution decomposes slowly with formation of a red solution, from which dark red crystals of **11** can be obtained. Yield: 0.48 g (62% relative to **4**). The products (P^tBu)$_4$[13] and $PH_2{}^tBu$ were detected by ^{31}P NMR spectroscopy (C_6D_6: δ −32.4 (s, ?), −59.0 (s, (P^tBu)$_4$), −80.1 (t, $PH_2{}^tBu$, $^1J_{P-H} = 174$ Hz)).

Table 4. Crystal Data and Structure Refinement Details for 5, 8, and 11

	5	**8**	**11**
formula	$C_{20}H_{30}Cl_2SiZr$	$C_{13}H_{14}Cl_2Zr$	$C_{13}H_{14}Cl_2Ti$
M_r	460.65	332.38	289.04
temp (K)	220(2)	213(2)	220(2)
cryst syst	monoclinic	monoclinic	monoclinic
space group	$C2/c$ (No. 15)	$P2_1/m$ (No. 11)	$P2_1/m$ (No. 11)
a (Å)	15.454(3)	7.118(1)	7.102(2)
b (Å)	12.219(2)	8.831(1)	8.604(4)
c (Å)	11.135(2)	10.163(1)	9.967(3)
β (deg)	105.05(3)	90.49(1)	90.67(2)
V (Å^3)	2030.5(6)	638.84(3)	609.0(3)
Z	2	2	2
ρ_{calcd} (Mg m^{-3})	1.507	1.790	1.576
F(000)	952	344	296
cryst size (mm)	0.5 × 0.4 × 0.3	0.5 × 0.4 × 0.3	0.4 × 0.2 × 0.1
abs coeff (mm^{-1})	0.864	1.251	1.108
$2\theta_{max}$ (deg)	4.3−56.1	4.0−55.5	4.1−54.7
no. of rflns collected	10942	3565	2666
no. of indep rflns	2306	1466	1313
R_{int}	0.0286	0.0264	0.0173
no. of params	170	112	112
R ($I > 2\sigma(I)$)	0.0247	0.0227	0.0282
wR2 (all data)	0.0626	0.0609	0.0836
$(\Delta/\rho)_{min}$ (e Å^{-3})	−0.374	−0.396	−0.328
$(\Delta/\rho)_{max}$ (e Å^{-3})	0.330	0.367	0.436

[{(η-C_5H_4)CMe_2PHPh}$_2$TiCl] (9). ^{31}P NMR (C_6D_6): δ 18.4 (d, $^1J_{P-H} = 212.0$ Hz). EI-MS: *m/z* 513 (7) [M$^+$], 297 (20) [M$^+$ − $C_5H_4Me_2PHPh$], 260 (75) [M$^+$ − 2 Ph], 216 (25) [$C_5H_4CMe_2PHPh^+$], and fragmentation thereof. IR (KBr): ν (cm^{-1}): 2287 m (ν(PH)), 1579 m (ν(C=C)), 1569 m (ν(C=C)). EPR: see Table 1.

[{(η-C_5H_4)CMe_2PH^tBu}$_2$TiCl] (10). ^{31}P NMR (C_6D_6): δ 38.6 (d, $^1J_{P-H} = 195.0$ Hz). EI-MS: *m/z* 473 (2) [M$^+$], 385 (10) [M$^+$ − P^tBu], 296 (12) [M$^+$ − 2 P^tBu], 260 (12) [(C_5H_4)$_2$$CMe_2Ti^+$], and fragmentation thereof. IR (KBr): ν (cm^{-1}): 2282 m (ν(PH)), 1471 s (ν(C=C)), 1261 s (ν(C=C)). EPR: see Table 1.

[{(η-C_5H_4)$_2$$CMe_2$}$TiCl_2$] (11). ^{1}H NMR ($CDCl_3$): δ 6.90 (t, 4H, C*H* in C_5H_4, $^3J_{H-H} = 2.5$ Hz), 5.55 (t, 4H, C*H* in C_5H_4, $^3J_{H-H} = 2.5$ Hz), 1.74 (s, 6H, CH_3). ^{13}C NMR ($CDCl_3$): δ 132.08 (s, 4C, C_5H_4), 116.42 (s, 2C, *ipso*-C in C_5H_4), 111.86 (s, 4C, C_5H_4), 37.77 (s, 1C, *C*−CH_3), 24.11 (s, 2C, C−*C*H_3). EI-MS: *m/z* 288 (28) [M$^+$], 252 (30) [M$^+$ − Cl], 237 (10) [M$^+$ − Cl − Me]. Anal. Calcd for $C_{13}H_{14}TiCl_2$ (289.04): C, 54.0; H, 4.8. Found: C, 53.8; H, 4.7.

X-ray Crystal Structure Determination of 5, 8, and 11. Data (λ(Mo Kα) = 0.710 73 Å) were collected with a Siemens CCD (SMART) diffractometer. All observed reflections were used for refinement (SAINT) of the unit cell parameters. Empirical absorption correction was carried out with SADABS.[31] The structures were solved by direct methods (SHELXTL PLUS).[32] Zr, Ti, Si, Cl, and C atoms were refined anisotropically; H atoms were located by difference maps and refined isotropically. Table 4 lists crystallographic details. Crystallographic data (excluding structure factors) for the structures reported in this paper have been deposited with the Cambridge Crystallographic Data Centre (**5**, CCDC-133344; **8**, CCDC-133345; **11**, CCDC-133346). Copies of the data can be obtained free of charge on application to The Director, CCDC, 12 Union Road, Cambridge, CB2 1EZ, U.K. (fax, int. code +(1223)336-033; e-mail, deposit@ccdc.cam.ac.uk).

---

(31) Sheldrick, G. M. SADABS—A Program for Empirical Absorption Correction; University of Göttingen, Göttingen, Germany, 1998.

(32) SHELXTL PLUS, Siemens Analytical X-ray Instruments Inc., 1990: XS, Program for Crystal Structure Solution; XL, Program for Crystal Structure Determination; XP, Interactive Molecular Graphics.

Acknowledgment. We gratefully acknowledge financial support from the *Fonds der chemischen Industrie*, the *Alexander von Humboldt-Foundation* (F.B.S.), the *Landesgraduiertenförderung Sachsen* (S.B.) and the *German-Israeli Foundation* (Grant No. I-142/95).

Supporting Information Available: Tables giving X-ray crystal structure data for **5**, **8**, and **11**. This material is available free of charge via the Internet at http://pubs.acs.org.

OM990763Z